




ORIGINAL RESEARCH

A novel three-step process for the identification of inner ear malformation types

Anandhan E. Dhanasingh Dr. rer. nat, MBA^{1,2}  | Nora M. Weiss Priv.-Doz. Dr³ |
 Varachaya Erhard MSc¹ | Fahad Altamimi MD^{4,5} | Peter Roland MD⁶ |
 Abdulrahman Hagr MBBS, FRCS (C)⁷ | Vincent Van Rompaey MD, PhD^{2,8}  |
 Paul Van de Heyning MD, PhD^{2,8} 

¹Research and Development Department, MED-EL, Innsbruck, Austria

²Department of Translational Neurosciences, Faculty of Medicine and Health Sciences, University of Antwerp, Antwerp, Belgium

³Department of Otorhinolaryngology-Head and Neck Surgery, Ruhr-University Bochum, St. Elisabeth-Hospital Bochum, Bochum, Germany

⁴Cochlear Implant Center, King Saud Medical City, Riyadh, Saudi Arabia

⁵Otolaryngology Head and Neck Surgery, College of Medicine, Alfaisal University, Riyadh, Saudi Arabia

⁶Department of Otolaryngology-Head & Neck Surgery, University of Texas Southwestern Medical Center, Dallas, Texas, USA

⁷King Abdullah Ear Specialist Center (KAESC), King Saud University, Riyadh, Saudi Arabia

⁸Department of Otorhinolaryngology and Head & Neck Surgery, Antwerp University Hospital, Antwerp, Belgium

Correspondence

Anandhan E. Dhanasingh, Research and Development Department, MED-EL Medical Electronics, Fürstenweg 77a, 6020 Innsbruck, Austria.

Email: anandhan.dhanasingh@medel.com

Nora M. Weiss, Department of Otorhinolaryngology-Head and Neck Surgery, Ruhr-University Bochum, St. Elisabeth-Hospital Bochum, Bochum, Germany.

Email: nora.weiss@rub.de

Funding information

MED-EL GmbH

Abstract

Objective: We hypothesize that visualizing inner-ear systematically in both cochlear view (oblique coronal plane) and in mid-modiolar section (axial plane) and following three sequential steps simplifies, identification of inner-ear malformation types.

Methods: Pre-operative computer-tomography (CT) scans of temporal bones of 112 ears with various inner ear malformation (IEM) types were taken for analysis. Images were analyzed using DICOM viewers, 3D slicer, and OTOPLAN[®]. The inner-ear was captured in the oblique-coronal plane for the measurement of length and width of cochlear basal turn which is also called as A-, and B-values respectively (Step 1). In the same plane, the angular-turns of lateral-wall (LW) of cochlear basal turn were measured (Step 2). As Step 3, the mid-modiolar section of inner ear was captured in the axial plane by following the A-value and perpendicular to cochlear view. From the mid-modiolar section, the outer-contour of inner ear was captured manually by following contrasting gray area between fluid filled and bony promontory and was compared to known resembling objects to identify IEM types (Step 3).

Results: Following reference values have emerged from our analysis: A-, and B-values (Step 1) on average are >8 mm and >5.5 mm respectively, in normal cochleae (NA), enlarged vestibular aqueduct syndrome (EVAS), incomplete partition (IP) type-I and -II, whereas it is <8 mm and <5.5 mm respectively, in IP type-III and cochlear hypoplasia (CH). Angular-turn of LW is consistently observed in cochlear basal turn (Step 2), is 540° in NA and EVAS, 450° in IP-II, and 360° in IP types I & III. In subjects with CH type, angular-turn of LW is either 360° or 450° or 540°. In true mid-modiolar section, outer-contour of inner-ear (Step-3), other than in CH and cystic inner-ear malformations, resembles recognizable shapes of known objects. Absence of EVA is an additional characteristic that confirms diagnosis of CH when the A-, B-values, and angular-turn of LW can be similar to other anatomical types. Drawing a straight line

Anandhan E. Dhanasingh and Nora M. Weiss contributed equally to this study.

This is an open access article under the terms of the [Creative Commons Attribution-NonCommercial-NoDerivs](https://creativecommons.org/licenses/by-nc-nd/4.0/) License, which permits use and distribution in any medium, provided the original work is properly cited, the use is non-commercial and no modifications or adaptations are made.

© 2022 The Authors. *Laryngoscope Investigative Otolaryngology* published by Wiley Periodicals LLC on behalf of The Triological Society.

along posterior edge of internal auditory canal (IAC) in axial view can differentiate a true common cavity (CC) from cochlear aplasia-vestibular cavity (VC).

Conclusion: Three-step process proposed in this study captures inner-ear in cochlear view as well in mid-modiolar sections visualizing key features of inner-ear in identification of IEM types.

Level of Evidence: Level 1.

KEYWORDS

cochlear view, imaging, inner ear malformation, lateral wall, mid-modiolar section

1 | INTRODUCTION

Inner ear malformation (IEM) has been reported worldwide at a rate of 20%–30% among children with congenital hearing loss.^{1,2} Detailed radiological analysis is necessary to identify the unique characteristics seen in each IEM type that differentiates from other types.³ Enlarged vestibular aqueduct (EVA) in EVA syndrome and, along with cystic apex, is seen in incomplete partition (IP) type II (IP-II). In IP type I (IP-I), the cochlear portion is completely cystic, but separated from the vestibular portion. A wide internal auditory canal (IAC) that opens up fully to the cochlear basal turn, along with a steep spiraling of the cochlear turns, is characteristic of IP type III (IP-III). A single cyst can represent either a common cavity (CC) with both a cochlear and vestibular portion or a vestibular cavity alone (VC) with cochlear aplasia (CA). Cochlear hypoplasia (CH) is identified by its smaller size.⁴ Cochlear implant (CI) electrode insertion complications in IEM include inadvertent electrode insertion into the IAC, electrode tip fold-over⁵ and partial insertion of longer electrodes in CH.⁶ Gushing, which is a severe outflow and oozing which is a mild outflow of cerebrospinal fluid, upon opening the cochlea are surgical complications associated with several IEMs.⁷

Identification of different IEM types may help the operating surgeon to limit surgical and CI electrode insertion complications.⁸ In our previous study, we reported an average diameter of the cochlear basal turn (A-value) <8 mm for IP-III and CH, whereas it is >8 mm among those with normal anatomy (NA), EVAS, IP-II, and IP-I.⁹ It was concluded that the A-value alone cannot be a predictor of the IEM types. In another previous study, we visually analyzed the outer contour of the true mid-modiolar section of the inner ear and identified unique patterns resembling known objects for every IEM type.⁴

The current study, (i) investigates a new method of analyzing the cochlear basal turn in a single image slice, addressing the angular turn to which the lateral wall (LW) is visible and (ii) analyses whether it might help identify different IEM types.

It is hypothesized, which is a projection of the inner ear into both the oblique coronal plane of the cochlear basal turn or also called as “cochlear view,”¹⁰ as well the true mid-modiolar section in the axial plane, is feasible using any advanced digital imaging and communications in medicine (DICOM) viewers including the clinically approved otologic planning tool (OTOPLAN[®]). This study aims, (i) to investigate a novel three-step process for the identification of IEM types and (ii) to create a master flowchart to enable its application for users.

2 | MATERIALS AND METHODS

2.1 | Image analyses

Pre-operative computer-tomography (CT) scans of temporal bones of 112 ears of potential CI candidates with various inner ear anatomical types were retrieved from the image database of King Abdullah Ear Specialist Center, King Saud University, between 2016 and 2021. From the radiological report, we found that the images were obtained using a 512-slice multidetector-row CT scanner (General Electric Healthcare). The following scanning parameters were used: axial plane, 0.625 mm slice thickness, 230 mAs, 140 kV, and rotation time 1 s with 0.3 mm reconstruction in the axial and coronal views. This retrospective study was approved by the Institutional Review Board (No. 20/0091/IRB) on November 30, 2020, to use the images for research purpose after anonymization. The CT images were analyzed using three-dimensional (3D) slicer, version 4.11.1 (www.slicer.org), and OTOPLAN[®] (<https://www.cascination.com/en/otoplan>) by the authors (Anandhan E. Dhanasingh, Nora M. Weiss, and Varachaya Erhard) together to reach a consensus on the observations made on the below given three-step process in the identification of IEM types.

Prior to the application of the three-step process, the authors (Peter Roland and Abdulrahman Hagr) have several years of experience in cochlear implantation field, analyzed the CT scans of temporal bone and classified it under different inner ear anatomical types following the method described by Sennaroglu et al.¹

2.1.1 | Three-step process in the identification of IEM types

Step 1: The A- and B-values were measured in the cochlear view projection as previously described by Escude et al.¹¹ (Figure 1A). The A-value was measured starting at the round window opening. It passes through the center of the cochlea to the opposite side of the LW. The B-value was measured perpendicular to the A-value and establishes the length of the short axis.

Step 2: The angular turn to which the LW of the cochlea can be followed in a single image slice corresponding to the cochlear view showing the cochlear basal turn is depicted in Figure 1B. The cross-hair feature which is the intersection of the A- and the B-value lines

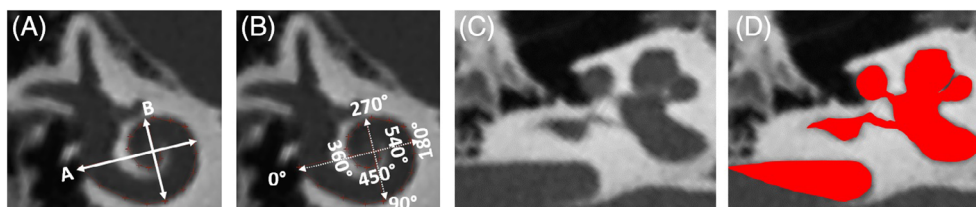


FIGURE 1 Oblique coronal view/cochlear view showing the cochlear basal turn diameter (A-value) and the width (B-value) measurements (A), angular turn of the lateral-wall traced manually in the single image slice (B), inner ear visualized in the true mid-modiolar section (c), captured outer contour of the inner ear (d)

divides the cochlear basal turn into quadrants of 90°, which is helpful in following the angular turn of the LW.

Step 3: Along the A-value line and perpendicular (90°) to the cochlear view, the mid-modiolar section of the inner ear was visualized in the axial plane as previously described by Dhanasingh et al.⁴ The outer contour of the mid-modiolar section of the inner ear in the axial view was captured manually by following the contrasting gray area between the fluid filled and bony region as previously described by Dhanasingh et al.¹² (Figure 1C).

The proposed three-step process was performed in both OTOPLAN® and in standard DICOM viewer (3D slicer) by the authors (Anandhan E. Dhanasingh, Nora M. Weiss), and was scrutinized by all the other authors.

2.2 | Statistical analyzes

The A- and B-values of the all the anatomical types were compared using two sample *t*-tests with unequal variance in Microsoft Excel for Office 355 (Version 2020). A $p < .05$ was considered statistically significant with a confidence interval of 95%. Statistical analysis on the angular depth of LW traced in the cochlear view for different anatomical types was not possible as the angular depth measured was uniform among the anatomical types.

3 | RESULTS

3.1 | Demographics

Table 1 lists the anatomical types identified, number of ears analyzed per anatomical type, mean A-, B-values along with its range, and the extent to which the LW can be consistently traced in the “cochlear view” in terms of angular turns.

The number of CT scans with various anatomical types identified in this study from the university database is more than the previous study.⁹ One sample was more in NA type, 14 samples were more in EVAS type, two samples were more in IP-II type, 12 samples were more in IP-I type, one sample was more in IP-III type and four samples were more in CH type. No change in the number of samples in CC and VC types.

3.2 | Identification of IEM types

3.2.1 | Step 1: Measurement of A-, B-values

The A- and B-values of various anatomical types other than CC and VC types are listed in Table 1. The A-values of all ears with IP-III and CH types were <8 mm compared to other types in which the A-values of all ears was >8 mm. The A-values of all ears with IP-III and CH types were significantly different compared to all ears with NA ($p < .001$; $p < .01$) and EVAS ($p < .0001$; $p < .01$) types. A-values of IP-III type was significantly different to IP-II ($p = .04$) and IP-I ($p = .01$) types. However, the A-values of CH type did not differ significantly from IP-I and IP-II ($p = .36$; $p = .11$) types. The B-values of all ears with IP-III, and CH types were <5.5 mm compared to all ears with other IEM types in which the B-value was >5.5 mm. The B-values of all ears with IP-III and CH types were significantly different compared to all ears with NA ($p < .0001$; $p < .001$) and EVAS ($p < .0001$; $p < .01$) types. B-values of all ears with IP-III type were significantly different to IP-II type ($p < .01$). However, the B-values of all ears with CH type did not differ significantly from all ears with IP-I ($p = .18$) and IP-II ($p = .02$) types. The A- and B-value measurements of all ears with CC and VC types were not possible due to the cystic appearance with no clear anatomical landmarks.

3.2.2 | Step 2: Angular turn of the LW of the cochlear basal turn

Captured in the cochlear view, the angular turn of the LW of the cochlear basal turn was identified at least 540° consistently in all ears with NA and EVAS types (Figure 2A,B), which is clearly higher than the angular turn of the LW of the cochlear basal turn of all ears with other anatomical types. Within the cochlear view, the LW was seen tightly curled beyond 360° to 540° of angular turn in NA type, whereas the LW was not seen tightly curled in EVAS type. In IP-I (Figure 2C) and IP-III (Figure 2E) types, angular turn of the LW was 360° as visually observed, whereas in IP-II type (Figure 2D), it extended to 450° as visually observed on a consist basis. These visual observations were uniformly seen by all three observers in all CT scans within each of the anatomical types other than CH type taken for analysis. In CH type, a large variation was seen in the angular turn

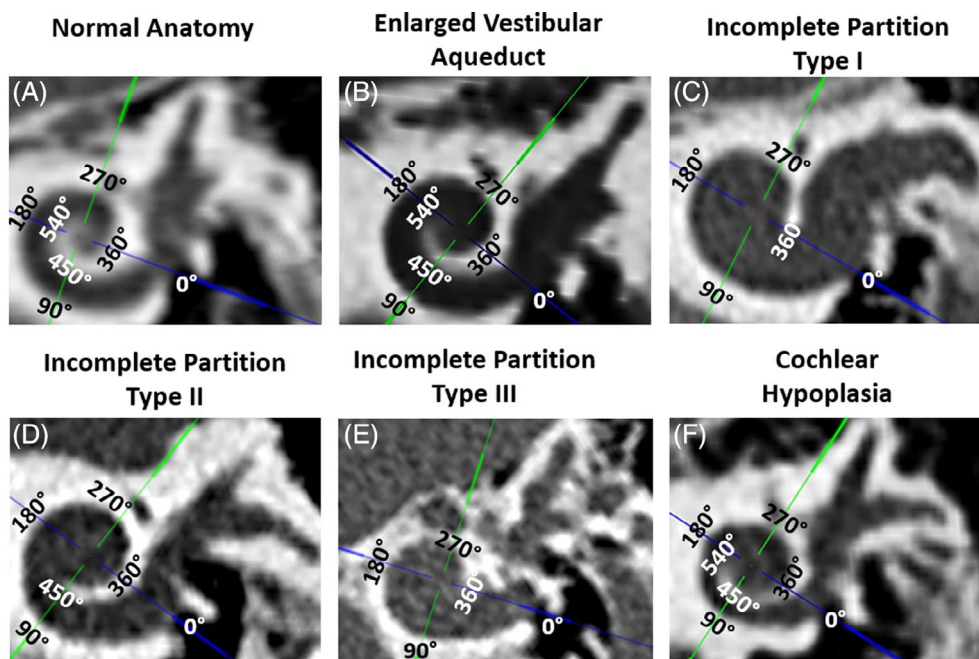
TABLE 1 Anatomical types of the inner ear identified along with the A- and B-values and the angular depth of the lateral wall traced

| Anatomical types (no. of CT scans) | A-value (mm) | | B-value (mm) | | Angular depth of LW traced (°) |
|------------------------------------|--------------|----------|--------------|---------|--------------------------------|
| | Mean (SD) | Range | Mean (SD) | Range | |
| NA (11) | 9.0 (0.6) | 8.1–10.1 | 6.6 (0.5) | 5.8–7.7 | 540° |
| EVAS (24) | 8.8 (0.4) | 8.2–9.5 | 6.2 (0.3) | 5.3–6.7 | 540° |
| IP-II (12) | 8.4 (0.7) | 7.6–9.7 | 6.1 (0.5) | 5.5–7.0 | 450° |
| IP-I (22) | 8.3 (0.5) | 7.3–9.5 | 5.6 (0.6) | 4.2–6.5 | 360° |
| IP-III (11) | 7.9 (0.4) | 7.4–8.5 | 5.2 (0.5) | 4.5–6.1 | 360° |
| CH (14) | 7.8 (1.1) | 6.6–9.4 | 5.2 (1.1) | 3.2–6.9 | 360°/450°/540° |
| Classic CC (8) | - | - | - | - | - |
| VC (10) | - | - | - | - | - |

Note: The order of the anatomical types given below are based on in the ascending order of severity.

Abbreviations: CC, common cavity; CH, cochlear hypoplasia; EVAS, enlarged vestibular aqueduct syndrome; IP, incomplete partition; LW, outer wall length; NA, normal anatomy; SD, standard deviation; VC, vestibular cavity.

FIGURE 2 Angular turn of the lateral-wall traced manually with the help of cross-hair feature (screenshots from OTOPLAN®) from different inner ear malformation types other than common cavity and vestibular cavity. Normal anatomy (A), enlarged vestibular aqueduct (B), incomplete partition type I (C), incomplete partition type II (D), incomplete partition type III (E), and Cochlear hypoplasia (F)



of the LW was visually observed. The angular turn of the LW of 540° was observed in four ears, 450° in three ears, and 360° in seven ears, respectively. Figure 2F captures one sample within CH type showing the angular turn of the LW of 540°.

CC and VC types were either elliptical or irregularly shaped in the cochlear view, with a cystic appearance as shown in Figure 3.

3.2.3 | Step 3: Visual observation of the outer contour of the inner ear captured in the mid-modiolar section

The outer contours of various anatomical inner ear samples captured in the mid-modiolar section are shown in Figure 4. NA and EVAS resembled Aladdin's lamp with EVAS showing an EVA. In addition, IP-I resembled the Sphinx and pyramid behind, IP-II the profile of the

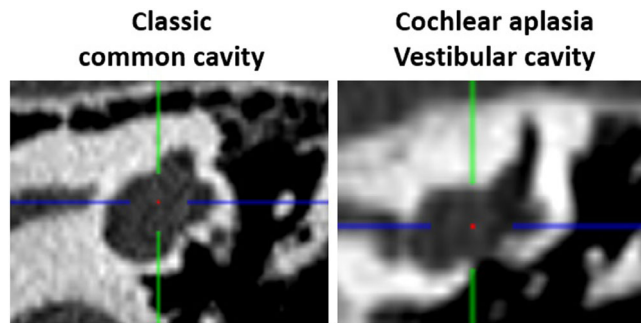


FIGURE 3 The cochlear view of a classic common cavity and a vestibular cavity showing a cystic appearance

Pomeranian dog's face, and IP-III an auger screw tip. The CH type appeared different to all the other anatomical types with no clear resemblance of any known object.

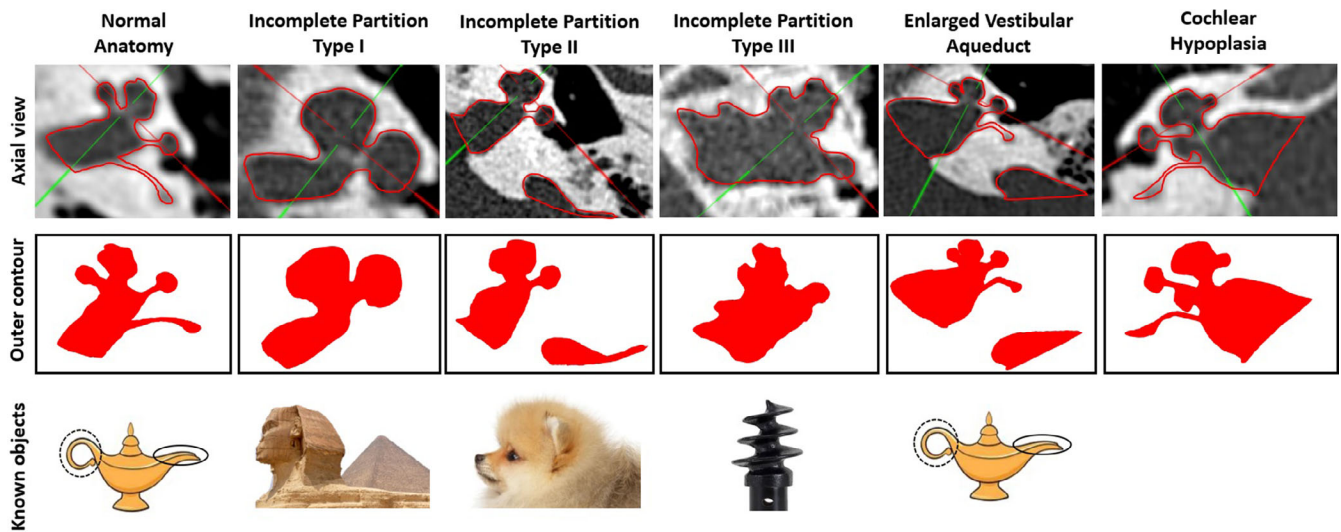


FIGURE 4 Axial view captured in OTOPLAN[®] showing the mid-modiolar section of the various anatomical types of inner ear malformations (top panel), outer contour of the mid-modiolar section of the inner ear (middle panel), and the known objects resembling the outer contour (bottom panel).

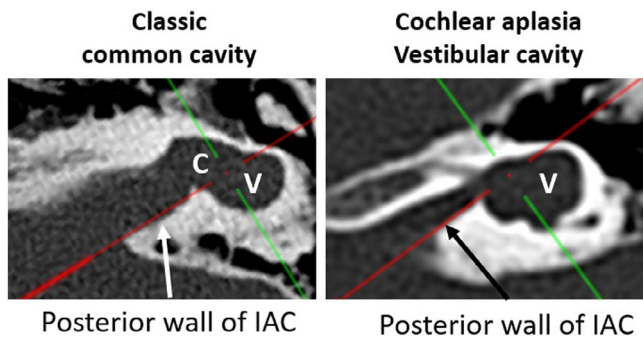


FIGURE 5 Red line drawn along the posterior edge of the internal auditory canal in the axial view from OTOPLAN[®] distinguishes the cochlear (C) and the vestibular portion (V) in classic common cavity from the isolated vestibular portion in cochlear aplasia vestibular cavity.¹³

Within the single cavity type, the line drawn along the posterior wall of the IAC seen in the axial view differentiates the CC when the line passes through the cavity separating the cochlear portion above the line and the vestibular portion below the line. In CA with VC, the cavity lies beyond the straight line. Figure 5 shows the axial view of the cystic type of inner ear with the red line of the cross-hair drawn along the posterior edge of the IAC in the axial view.

3.3 | Flowchart for identifying IEM types

Based on the above findings, the flowchart shown in Figure 6 describes a three-step sequential process for the accurate identification of IEM types. In Step 1, the A-value measured from the cochlear view is used to approximately differentiate NA, EVAS, IP type I, and II

types (>8 mm) from IP-III and CH types (<8 mm). The B-value measured from the cochlear view can also approximately differentiate NA, EVAS, IP type I, and II types (>5.5 mm) from IP-III and CH types (<5.5 mm). However, both the A- and B-values alone cannot confirm the anatomical types accurately as the A-value range extend up to 8.5 mm in IP type III and 9.4 mm in CH type and the B-value range extend up to 6.1 mm in IP-III and 6.9 mm in CH types. Step 1 is mandatory to obtain the cochlear view to perform Step 2. In Step 2, in the cochlear view, an angular turn of LW of 540° was determined as the cut-off value to differentiate NA, EVAS, and CH types from other anatomical types. An angular turn of LW of 450° may indicate IP-II or CH types. Whereas, an angular depth of LW of 360° may indicate IP-I, IP-III or CH types. In Step 3, the true mid-modiolar section of the inner ear is obtained by cutting the cochlea through the A-value line created in the cochlear view to get the optimal axial view. The outer contour of the mid-modiolar section of the inner ear resembling Aladdin's lamp from Step 3 together with the 540° of angular turn of the LW in the cochlear view from Step 2 confirms NA type. The outer contour of the mid-modiolar section of the inner ear resembling Aladdin's lamp from Step 3 together with EVA and 540° of angular turn of LW in the cochlear view from Step 2 is a strong indicator for EVAS. The outer contour resembling the profile of Pomeranian dog face together with EVA from Step 3 and 450° of angular turn of LW in the cochlear view from Step 2 is a strong indicator for IP-II. The Sphinx Pyramid resemblance of the outer contour of the mid-modiolar section from Step 3, together with 360° angular turn of LW in the cochlear view is a strong indicator for IP-I type. An auger screw tip resemblance of the outer contour of the mid-modiolar from Step 3 section together with 360° angular turn of LW in the cochlear view is a strong indicator for IP-III type. Any angular turn (360°, 450°, or 540°) in the cochlear view together with an outer contour of the mid-modiolar section that does not resemble any of the known objects

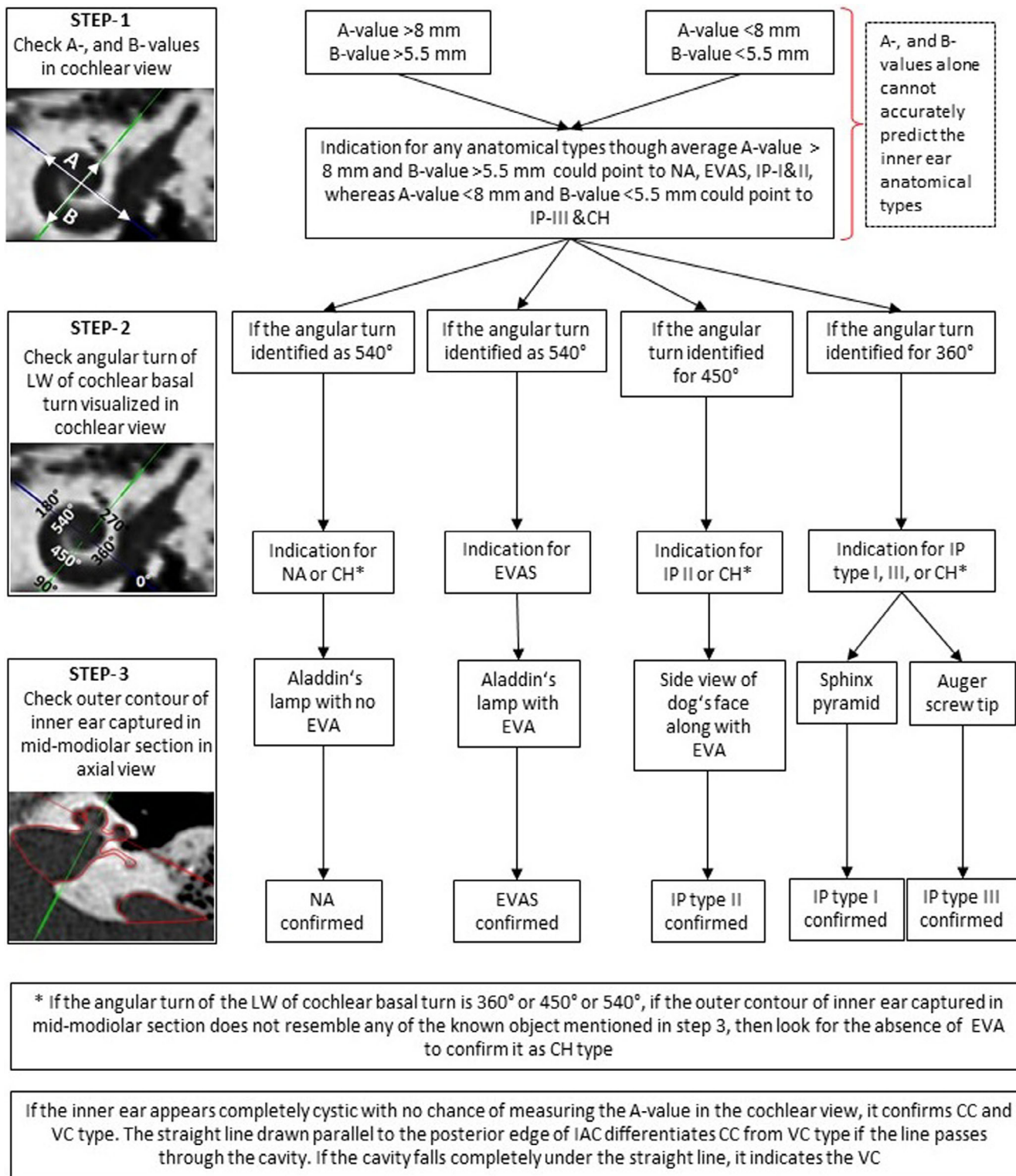


FIGURE 6 Suggested flowchart illustrating the sequential steps to follow in the identification of the inner ear anatomical types

mentione and showing a clear absence of EVA may indicate CH. The cystic type of inner ear is easily distinguishable from other anatomical types. The line drawn along the posterior edge of IAC as visualized in the axial view (mid-modiolar section) separating the cochlear and the vestibular portion helps to differentiate classic CC from VC type.

4 | DISCUSSION

Identification of IEM types helps place the CI electrode optimally and to effectively minimize the surgical complications that are characteristics of certain IEM types. This study aimed to develop

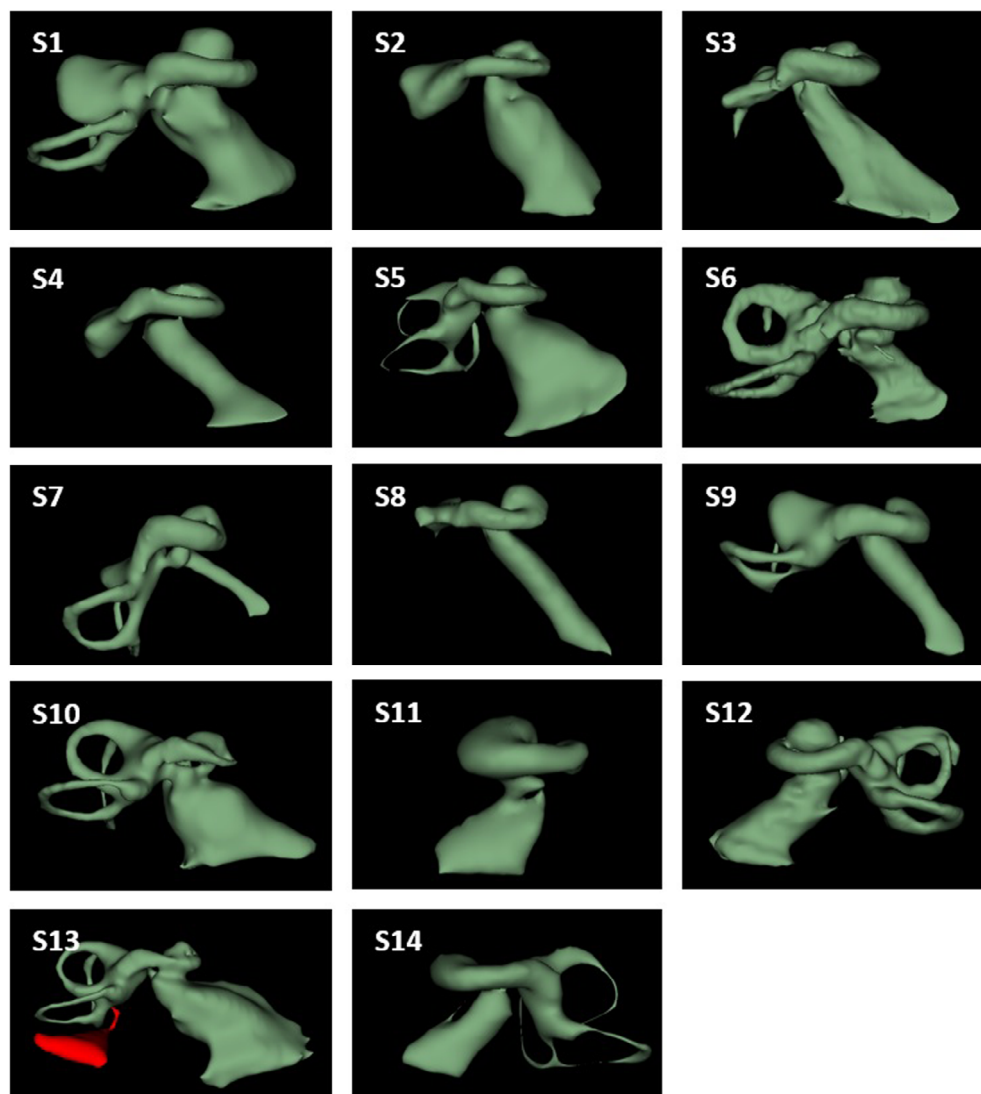


FIGURE 7 Fourteen samples within cochlear hypoplasia type in the axial view to visualize the appearance of the vestibular portion. Samples S2, S3, S4, S8, and S11 shows the absence of vestibular portion. Samples S1, S7, and S9 shows underdeveloped lateral semi-circular canal. Samples S5, S6, S10, S12, S13, and S14 shows the normal presence of the vestibular portion.

an effective and comprehensive method to identify IEM types that can be applied by clinicians with any level of experience. A flowchart with three sequential steps to identify IEM types is presented.

The three sequential steps given in the flowchart to identify the anatomical types were successfully applied to all the 112 CT scans in this study. Previously,⁹ we reported on the A-value measurement in the cochlear view which is Step 1 of the current study. It is interesting to see the A-value is clinically measured even in the malformed type as recently reported by Wimmer et al. in 2022.¹⁴ In that report, IP type II was reported to have A-value of >8 mm which is in-line with the finding of this current study. Our earlier report on the observation of the outer contour of the mid-modiolar section of the inner ear is the Step 3 of the current study.⁴ The addition of new Step 2 now enables a systematic evaluation of the pre-operative images in the identification of different IEM types. The flowchart proposed for the identification of inner ear anatomical types was based on the observations made from all 112 CT scans, which itself can be considered as validation of the flowchart.

Discussing Step 2 in detail, the angulation of the LW captured in the single image slice corresponding to the cochlear view of the cochlear basal turn revealed that specific anatomical types have certain angular extension of the LW. The cross-hair function in the OTOPLAN[®] simplifies the observation of the angular extension of the LW and every quadrant corresponds to 90° of incrementation. The LW was angularly followed up to 540° consistently in the NA, EVAS, and CH types, 450° in IP-II and CH types and 360° in IP-I, -III, and CH types. This was in consensus among all the three observers.

While most inner ear anatomical types can be identified either from the cochlear view or from the mid-modiolar section, CH needs more attention. The angular turn of the LW of the cochlear basal turn in the CH type is not uniform as seen in other anatomical types and the outer contour of the mid-modiolar section may resemble EVAS or IP-II. Consequently, the absence of EVA and distorted appearance of vestibular portion may help to differentiate CH as shown in Figure 7. Out of 14 CH samples, the vestibular portion was almost absent in five samples (S2, S3, S4, S8, and S11), lateral semicircular canal was underdeveloped in three samples (S1, S7, and S9) leaving the other six

samples with almost normal presence of the vestibular portion. 3D segmentation of the inner ear is a valuable tool specially to differentiate CH type, when the three-step process proposed in this study is inconclusive.

The very first classification of IEM types was proposed by Jackler et al. in 1987 based on the time of developmental arrest during embryogenesis.¹⁵ In 2002, Sennaroglu et al.¹⁶ reported radiological findings differentiating IP-I which is characterized by a cystic cochlear portion from IP-II which has a further developed cochlear basal turn with a cystic apex. In 2021, Grover et al.¹⁷ reported a new classification of cochleovestibular malformation by specifically looking at the cochlear morphology, the modiolus, and the lamina cribrosa without considering IEM types that are associated with EVA. None of these reports on the classification of IEM types involved any systematic manner of visualizing the inner ear in both cochlear view and the mid-modiolar section.

The current study reported a sample size of 112, which is big compared to previous reports¹⁴⁻¹⁶ and is considered sufficient to describe a classification of IEM types. The proposed step-by-step approach to evaluate pre-operative images enables a comprehensive approach in the identification of IEM types. Grover et al.,¹⁸ Thong et al.,¹⁹ and Alanazi et al.²⁰ reported of varying cochlear size based on ethnicity which needs to be critically considered in the lights of all 112 CT scans used in this study were from one particular geographical location. This is one of the limitations of this study and the proposed flowchart needs validation applying CT scans of inner with varying anatomical types from other geographical location and ethnicity.

5 | CONCLUSION

The systematic application of the three-step process proposed in this study is a novel method in the identification of IEM types. The visualizing inner ear in both cochlear view and the mid-modiolar section enables to capture every key anatomical structure of the inner ear in the identification of anatomical types.

FUNDING INFORMATION

The authors Anandhan E. Dhanasingh and Varachaya Erhard are employed at MED-EL GmbH within the research and development department. Nora M. Weiss received traveling grants from MED-EL GmbH. This study did not receive any additional funds either from MED-EL or from other institutions.

CONFLICT OF INTEREST

The authors Anandhan E. Dhanasingh and Varachaya Erhard are employed at MED-EL GmbH. This study did not carry any promotional content. All the other authors have declared no conflict of interest.

ORCID

Anandhan E. Dhanasingh  <https://orcid.org/0000-0003-2116-9318>

Vincent Van Rompaey  <https://orcid.org/0000-0003-0912-7780>

Paul Van de Heyning  <https://orcid.org/0000-0002-8424-3717>

REFERENCES

- Sennaroglu L, Bajin MD. Classification and current management of inner ear malformations. *Balkan Med J.* 2017;34(5):397-411. doi:10.4274/balkanmedj.2017.0367
- Sun B, Dai P, Zhou C. Study on 2,747 cases of inner ear malformation for its classification in patient with sensorineural hearing loss. *Lin Chung Er Bi Yan Hou Tou Jing Wai Ke Za Zhi.* 2015;29(1):45-47.
- Quirk B, Youssef A, Ganau M, D'Arco F. Radiological diagnosis of the inner ear malformations in children with sensorineural hearing loss. *BJR Open.* 2019;1(1):20180050. doi:10.1259/bjro.20180050
- Dhanasingh A, Erpenbeck D, Assadi MZ, et al. A novel method of identifying inner ear malformation types by pattern recognition in the mid modiolar section. *Sci Rep.* 2021;11(1):20868. doi:10.1038/s41598-021-00330-6
- Alsughayer L, Al-Shawi Y, Yousef M, Hagr A. Cochlear electrode array tip fold-over in incomplete partition-I - A case report. *Int J Pediatr Otorhinolaryngol.* 2020;139:110438. doi:10.1016/j.ijporl.2020.110438
- Widmann G, Dejaco D, Luger A, Schmutzhard J. Pre- and post-operative imaging of cochlear implants: a pictorial review. *Insights Imaging.* 2020;11(1):93. doi:10.1186/s13244-020-00902-6
- Bajin MD, Pamuk AE, Pamuk G, Özgen B, Sennaroglu L. The association between modiolar base anomalies and intraoperative cerebrospinal fluid leakage in patients with incomplete partition type-II anomaly: a classification system and presentation of 73 cases. *Otol Neurotol.* 2018;39(7):e538-e542. doi:10.1097/MAO.0000000000001871
- Aldhafeeri AM, Alsanosi AA. Management of surgical difficulties during cochlear implant with inner ear anomalies. *Int J Pediatr Otorhinolaryngol.* 2017;92:45-49. doi:10.1016/j.ijporl.2016.11.001
- Khurayzi T, Almuhas F, Alsanosi A, Abdelsamad Y, Doyle Ú, Dhanasingh A. A novel cochlear measurement that predicts inner-ear malformation. *Sci Rep.* 2021;11(1):7339. doi:10.1038/s41598-021-86741-x
- Xu J, Xu SA, Cohen LT, Clark GM. Cochlear view: postoperative radiography for cochlear implantation. *Am J Otol.* 2000;21(1):49-56.
- Escudé B, James C, Deguine O, Cochard N, Eter E, Fraysse B. The size of the cochlea and predictions of insertion depth angles for cochlear implant electrodes. *Audiol Neurotol.* 2006;11(Suppl 1):27-33. doi:10.1159/000095611
- Dhanasingh A, Dietz A, Jolly C, Roland P. Human inner-ear malformation types captured in 3D. *J Int Adv Otol.* 2019;15(1):77-82. doi:10.5152/iao.2019.6246
- Weiss NM, Langner S, Mlynski R, Roland P, Dhanasingh A. Evaluating common cavity cochlear deformities using CT images and 3D reconstruction. *Laryngoscope.* 2021;131(2):386-391. doi:10.1002/lary.28640
- Wimmer W, Soldati FO, Weder S, et al. Cochlear base length as predictor for angular insertion depth in incomplete partition type 2 malformations. *Int J Pediatr Otorhinolaryngol.* 2022;159:111204. doi:10.1016/j.ijporl.2022.111204
- Jackler RK, Luxford WM, House WF. Congenital malformations of the inner ear: a classification based on embryogenesis. *Laryngoscope.* 1987;97(3 Pt 2 Suppl 40):2-14. doi:10.1002/lary.5540971301
- Sennaroglu L, Saatci I. A new classification for cochleovestibular malformations. *Laryngoscope.* 2002;112(12):2230-2241. doi:10.1097/00005537-200212000-00019
- Grover M, Sharma S, Samdani S, et al. New SMS classification of cochleovestibular anomalies: our experience with 25 cases of type I anomaly. *Indian J Otolaryngol Head Neck Surg.* 2021;73(3):333-339. doi:10.1007/s12070-021-02442-x
- Grover M, Sharma S, Singh SN, Kataria T, Lakhawat RS, Sharma MP. Measuring cochlear duct length in Asian population: worth giving a thought! *Eur Arch Otorhinolaryngol.* 2018;275(3):725-728. doi:10.1007/s00405-018-4868-9

19. Thong JF, Low D, Tham A, Liew C, Tan TY, Yuen HW. Cochlear duct length-one size fits all? *Am J Otolaryngol*. 2017;38(2):218-221. doi:[10.1016/j.amjoto.2017.01.015](https://doi.org/10.1016/j.amjoto.2017.01.015)
20. Alanazi A, Alzhrani F. Comparison of cochlear duct length between the Saudi and non-Saudi populations. *Ann Saudi Med*. 2018;38(2):125-129. doi:[10.5144/0256-4947.2018.125](https://doi.org/10.5144/0256-4947.2018.125)

How to cite this article: Dhanasingh AE, Weiss NM, Erhard V, et al. A novel three-step process for the identification of inner ear malformation types. *Laryngoscope Investigative Otolaryngology*. 2022;7(6):2020-2028. doi:[10.1002/lio2.936](https://doi.org/10.1002/lio2.936)